

Enhancement and Suppression of the Neutrino-Nucleon Total Cross Section at Ultra-High Energies

Jamal Jalilian-Marian

Physics Department, Brookhaven National Laboratory, Upton NY 11973

Abstract

We argue that high gluon density effects at small x are important for the calculation of ultra-high energy neutrino nucleon cross sections due to the phenomenon of geometric scaling. We calculate the cross section for $\nu N \rightarrow \mu X$, including high gluon density effects, using the all twist formalism of McLerran and Venugopalan and show that it can be related to the dipole nucleon cross section measured in DIS experiments. For neutrino energies of $E_\nu \sim 10^{12}$ GeV, the geometric scaling region extends all the way up to $Q^2 \sim M_W^2$. We show that geometric scaling can lead to an *enhancement* of the neutrino nucleon total cross section by an order of magnitude compared to the leading twist cross section and discuss the implications for neutrino observatories. At extremely high energies, gluon saturation effects suppress the neutrino nucleon total cross section and lead to its unitarization.

1 Introduction

Ultra high energy neutrinos are a source of great mystery and excitement and offer a possible window onto phenomena beyond the standard model. Because of their weak interactions with matter, neutrinos can travel large distances and therefore carry information about very distant objects. The origins of ultra high energy neutrinos are uncertain and the subject of intense theoretical and experimental interest and investigation [1]. Some possible sources are active galactic nuclei, decays of super heavy particles and gamma ray bursts. They can be detected by measuring the air showers initiated by the muon produced in neutrino-nucleon interactions through a charged current.

The total neutrino nucleon cross section can be calculated [2] in the standard model using the various parametrizations of parton distribution functions [3] measured at HERA [4]. At very high neutrino energies, one needs to know the behavior of the parton distribution functions at small x . It can be shown that a power growth of the parton distribution functions with x would lead to a power growth of the neutrino nucleon total cross section with neutrino energy. This would eventually lead to the violation of unitarity at high energies.

Unitarization of ultra high energy neutrino nucleon cross sections has been of considerable interest lately [5, 6, 7, 8]. Saturation of the gluon distribution function at very small x [9] is expected to restore unitarity at high energies. One can make a rough estimate of the magnitude of unitarity corrections at a given neutrino energy by considering the first higher twist correction factor $\alpha_s x G(x, Q^2)/\pi R^2 Q^2$. Since the neutrino nucleon cross section is dominated by scales $Q^2 \simeq M_W^2$, the effective value of x is $\sim \frac{M_W^2}{2M_h E_\nu}$. At a neutrino energy of $E_\nu \sim 10^{12}$ GeV, this is an effect of only a few percent. However, due to the phenomenon of geometric scaling, it is too naive to conclude that higher twist (high gluon density) effects can be disregarded.

It is an experimental fact that the HERA data at small x (< 0.01) and all Q^2 show geometric scaling [10]. In other words, the DIS cross section depends on only one variable, $Q^2/Q_s^2(x)$ rather than two independent variables x and Q^2 . Here $Q_s^2(x)$ is the saturation scale of the nucleon, arising from high gluon density effects, which can be extracted from the HERA data [11]. Geometric scaling is a property and prediction of the all twist formulation of QCD evolution equations for DIS structure functions and cross sections at small x (high energy) in the kinematic region $Q^2 < Q_s^2$ [12, 13]. Recently, it has been shown that the nonlinear evolution equations for the structure functions at small x exhibit this geometric scaling property [14] (see also [15]) in the kinematic region beyond Q_s^2 . Roughly, this means that high gluon density effects, which are dominant at scales $Q^2 \leq Q_s^2$, influence observables at much higher scales $Q^2 \gg Q_s^2$. This was used in [16] to fit the RHIC data on pion spectra at $p_t^2 \gg Q_s^2$ and to reproduce the N_{part} scaling of the data.

In [14] the Q^2 region where geometric scaling holds is calculated to be

$$Q_{max}^2 \ll \left[\frac{Q_s^2(x)}{\Lambda_{QCD}^2} \right] Q_s^2(x) \quad (1)$$

The geometric scaling region for different neutrino energies is shown in Figure (1). For easy

reference, we also show M_W^2 . We have used the Golec-Biernat and Wüsthoff parametrization of the saturation scale such that

$$Q_s^2(x) \equiv Q_{s0}^2 (x_0/x)^\lambda \quad (2)$$

where $Q_{s0}^2 = 1.0 \text{ GeV}^2$, $x_0 = 3.0 \times 10^{-4}$ and $\lambda = 0.28$, $\Lambda_{QCD} = 0.2 \text{ GeV}$. Furthermore, since most of the contribution to the cross section comes from $Q^2 \sim M_W^2$, we have set $x = \frac{M_W^2}{2M_h E_\nu}$.

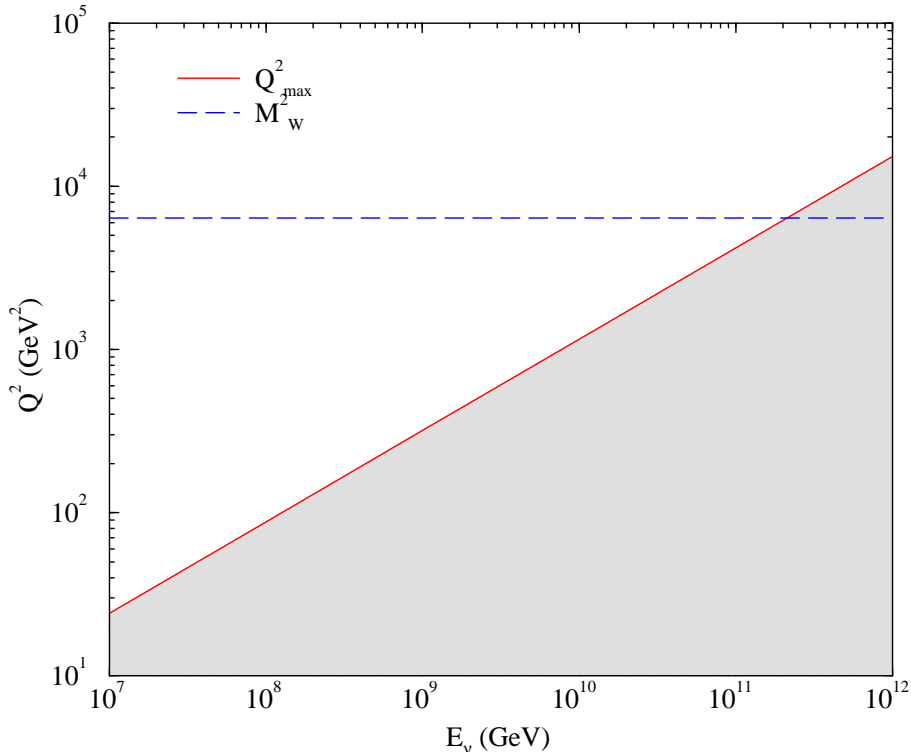


Figure 1: The geometric scaling region.

Clearly, by $E_\nu \sim 10^{12} \text{ GeV}$ we are in the geometric scaling region. Therefore, high gluon density and gluon saturation effects may be crucial. Since the standard expressions for the neutrino nucleon cross sections are calculated within the leading twist perturbative QCD formalism, they will break down due to the higher twist nature of gluon saturation. Here, we use the effective action and renormalization group approach to high energy QCD [12] to calculate this cross section including all higher twist (high gluon density) effects.

2 Neutrino nucleon cross section

In leading twist perturbative QCD, the expression for the neutrino nucleon differential cross section is given by

$$\frac{d^2\sigma^{\nu N}}{dx dQ^2} = \frac{G_F^2}{\pi} \left(\frac{M_{W,Z}^2}{Q^2 + M_{W,Z}^2} \right)^2 \left[q(x, Q^2) + (1 - Q^2/xs)^2 \bar{q}(x, Q^2) \right] \quad (3)$$

where x and Q^2 are the standard DIS variables and the quark and anti-quark distributions include the appropriate couplings for neutral and charged currents in DIS. To get the total cross section, one integrates over x and Q^2

$$\sigma_{total}^{\nu N}(s) = \int_0^1 dx \int_0^{xs} dQ^2 \frac{d^2\sigma^{\nu N}}{dx dQ^2} \quad (4)$$

At high neutrino energies and for very high values of $Q^2 \gg M_{W,Z}^2$, the integrand dies off quickly while shrinkage of the phase space kills the contribution from the low momentum ($Q^2 \ll M_{W,Z}^2$) region. Therefore, the dominant contribution to the total cross section comes from the region of $Q^2 \sim M_{W,Z}^2$ if one uses the standard parton distribution functions (by standard, we mean any of the available parametrizations of parton distributions such as MRS, CTEQ, GRV [3]).

At small x , higher twist effects become important. This means that the standard parton distribution functions, defined as the expectation values of certain two point operators get contributions from higher twist operators. This spoils their interpretation as a number density. One can still define and calculate physical observables such as the structure function F_2 [17] that are experimentally measured. However, one cannot relate the all twist structure functions to number distributions such as the standard gluon distribution function xG .

2.1 Charged current exchange

Here we use the effective action and classical field approach to high gluon density effects to calculate the cross section for the neutrino nucleon charged current interaction

$$\nu_\mu N \rightarrow \mu X \quad (5)$$

Since we will ignore all lepton masses, our results would also apply to electron and tau neutrino scattering. Also, in this work, we will ignore the neutral current exchange but it is quite similar to the process considered here. Our goal here is to derive an analytic expression for the above cross section such that it includes all higher twist effects that are expected to unitarize it.

We start with writing the differential cross section in terms of leptonic and hadronic tensors

$$\frac{d\sigma}{dx dQ^2} = \frac{1}{4\pi} \frac{y}{xs} \frac{G_F^2 M_W^4}{[Q^2 + M_W^2]^2} L^{\mu\nu}(k_1, k_2) W_{\mu\nu}(q^2, P \cdot q) \quad (6)$$

where k_1, k_2 are the incoming and outgoing lepton momenta, P is the nucleon momentum while $q = k_1 - k_2$ is the momentum transfer ($Q^2 = -q^2$). The leptonic tensor $L_{\mu\nu}(k_1, k_2)$

is standard and is not affected by high gluon density effects. It is

$$L^{\mu\nu}(k_1, k_2) \equiv 2 \left[k_1^\mu k_2^\nu + k_1^\nu k_2^\mu - g^{\mu\nu} k_1 \cdot k_2 + i \epsilon^{\mu\nu\rho\sigma} k_{1\rho} k_{2\sigma} \right] \quad (7)$$

The hadronic tensor $W_{\mu\nu}$ contains all the information about the high gluon density effect in a hadron. It is defined as

$$W_{\mu\nu}(q^2, P \cdot q) \equiv \frac{1}{2\pi} \text{Im} \int d^4 z e^{iqz} \langle P | T J_\mu^\dagger(z) J_\nu(0) | P \rangle \quad (8)$$

where $J_\mu \equiv \bar{u} \gamma_\mu (1 + \gamma_5) d$ is the charged weak current. The all twist hadronic tensor for electron proton DIS with a photon exchange has already been evaluated in [17]. Our calculation here is a straightforward generalization to W exchange relevant for the process considered here. Since we are working with a classical background field and external sources of color charge denoted by ρ , we will need to generalize (8). This was already done in [17] where the hadronic tensor is defined as

$$W_{\mu\nu} \equiv \frac{\sigma P^+}{2\pi M_h} \text{Im} \int dX^- \int d^4 z e^{iqz} \langle T J_\mu^\dagger(X^- + z/2) J_\nu(X^- - z/2) \rangle_\rho \quad (9)$$

where

$$\langle T J_\mu^\dagger(x) J_\nu(y) \rangle_\rho = \text{Tr} \gamma_\mu (1 + \gamma_5) S_u(x, y) \gamma_\nu (1 + \gamma_5) S_d(y, x) \quad (10)$$

and $S_{u,d}(x, y)$ is the u or d quark propagator in the background of the classical color field in coordinate space while σ is the target hadron transverse area and P^+ is the large component of the hadron momentum. In this approach, to calculate a physical quantity, one averages over color charges ρ at the end [12]. Despite its appearance, the hadronic tensor defined in (9) is Lorenz covariant as discussed in [17]. The propagator in the background field is given by¹ [17]

$$S(x, y) = S_0(x, y) - i \int d^4 r \left\{ \left[\theta(x^-) \theta(-y^-) [V^\dagger(r_t) - 1] - \theta(-x^-) \theta(y^-) [V(r_t) - 1] \right] S_0(x - r) \gamma^- \delta(r^-) S_0(r - y) \right\} \quad (11)$$

with the free fermion propagator given by

$$S_0(x - y) \equiv - \int \frac{d^4 p}{(2\pi)^4} e^{ip(x-y)} \frac{\not{p}}{p^2 - i\epsilon}. \quad (12)$$

$V(r_t)$ is a matrix in fundamental representation which includes the infinitely many gluon exchanges between the quark and the hadron. The propagator also has other pieces that involve θ functions on the same side in x^- and y^- . As shown in [17], these pieces are pure gauges and do not contribute to the cross section. Therefore, they are not included here.

¹Since we are ignoring quark masses, we will not distinguish between u and d quarks and we drop the flavor label from here on.

Finally, we will have to color average our results to get the physical cross sections. We will come back to this point later when we discuss dipole models.

Using eqs. (10) and (11) in (9) and after some lengthy algebra, we get

$$W_{\mu\nu} = \frac{N_c \sigma P^+}{2\pi M_h} \text{Im} \int \frac{d^4 p}{(2\pi)^4} \frac{d^4 k}{(2\pi)^4} (2\pi) \delta(k^-) \tilde{\gamma}(x, k_t, b_t) \frac{M_{\mu\nu}}{p^2 (p-k)^2 (p-q)^2 (p-q-k)^2} \quad (13)$$

where

$$\tilde{\gamma}(x, k_t, b_t) \equiv \int d^2 r_t e^{ik_t \cdot r_t} \gamma(x, r_t, b_t) \quad (14)$$

with

$$\gamma(x, r_t, b_t) \equiv \frac{1}{N_c} \text{Tr} \left[\left\langle 1 - V(b_t + \frac{r_t}{2}) - V^\dagger(b_t - \frac{r_t}{2}) + V(b_t + \frac{r_t}{2}) V^\dagger(b_t - \frac{r_t}{2}) \right\rangle_\rho \right] \quad (15)$$

and

$$M_{\mu\nu} \equiv 2 \text{Tr} (1 - \gamma_5) \gamma_\mu (\not{p} - \not{q} - \not{k}) \gamma^- (\not{p} - \not{q}) \gamma_\nu \not{p} \gamma^- (\not{p} - \not{k}) \quad (16)$$

The function $\gamma(x, r_t, b_t)$ is related to the (quark-antiquark) dipole-nucleon scattering amplitude in coordinate space.

To get the imaginary part of the hadronic tensor, we use the Landau-Cutkosky cutting rules. There are two distinct ways of cutting the diagram as shown in Fig. (2). The dotted lines are W boson gauge fields while the thin solid lines represent fermions. The thick solid lines with a filled circle represent insertion of the classical field and the thick dashed lines represent the possible cuts. The cuts where both classical field insertions are on the same side are not kinematically allowed. The cut propagator is put on shell along with a theta

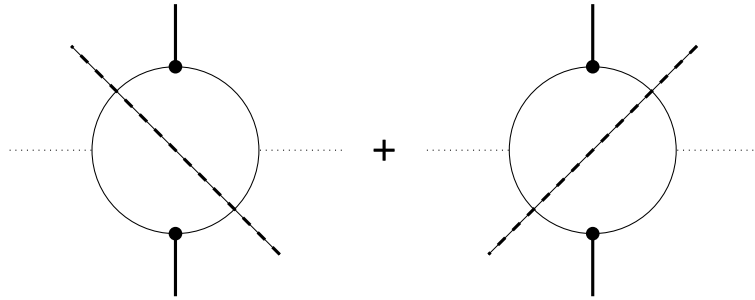


Figure 2: Imaginary part of the hadronic tensor.

function to ensure positive (negative) energy for fermions (antifermions). The sum of the two cuts is proportional to

$$\frac{\theta(p^+) \theta(q^+ - p^+ + k^+) \delta(p^2) \delta((p-k-q)^2)}{(p-k)^2 (p-q)^2} + \frac{\theta(p^+ - k^+) \theta(q^+ - p^+) \delta((p-k)^2) \delta((p-q)^2)}{p^2 (p-k-q)^2}$$

It is straightforward to show that the two contributions are actually equal with appropriate change of variables and $\mu \leftrightarrow \nu$. We get

$$W_{\mu\nu} = \frac{2N_c\sigma}{2\pi} \frac{P^+}{M_h} \int \frac{d^4p}{(2\pi)^4} \frac{d^4k}{(2\pi)^4} (2\pi)\delta(k^-) \tilde{\gamma}(x, k_t, b_t) M_{\mu\nu} \\ \times \frac{\theta(p^+ - k^+)\theta(q^+ - p^+)(2\pi)\delta((p-k)^2)(2\pi)\delta((p-q)^2)}{p^2(p-k-q)^2} \quad (17)$$

where

$$M_{\mu\nu} \equiv \text{Tr} \left[(1 - \gamma_5) \gamma_\mu (\not{p} - \not{q} - \not{k}) \gamma^- (\not{p} - \not{q}) \gamma_\nu \not{p} \gamma^- (\not{p} - \not{k}) \right. \\ \left. + (1 - \gamma_5) \gamma_\mu (\not{p} - \not{q}) \gamma^- (\not{p} - \not{q} - \not{k}) \gamma_\nu (\not{p} - \not{k}) \gamma^- \not{p} \right] \quad (18)$$

We can now use the delta functions to perform some of the integrals in (17). Defining $z \equiv p^-/q^-$, the effect of the theta functions is to restrict the z integration to the region between 0 and 1. We then get

$$M_h W_{\mu\nu} = \frac{N_c\sigma}{16\pi^2} \frac{2P \cdot q}{q^- q^-} \int_0^1 dz \frac{d^2p_t}{(2\pi)^2} \frac{d^2k_t}{(2\pi)^2} \tilde{\gamma}(x, k_t, b_t) \\ \frac{\{[M_{\mu\nu}^{sym} + \mu \leftrightarrow \nu] + [M_{\mu\nu}^{asym} - \mu \leftrightarrow \nu]\}}{[(p_t - zq_t)^2 - z(1-z)q^2][(p_t + k_t - zq_t)^2 - z(1-z)q^2]} \quad (19)$$

where $M_{\mu\nu}^{sym}$ and $M_{\mu\nu}^{asym}$ are now given by

$$M_{\mu\nu}^{sym} = \text{Tr} \gamma_\mu (\not{p} - \not{q} + \not{k}) \gamma^- (\not{p} - \not{q}) \gamma_\nu \not{p} \gamma^- (\not{p} + \not{k}) \quad (20)$$

and

$$M_{\mu\nu}^{asym} = -\text{Tr} \gamma_5 \gamma_\mu (\not{p} - \not{q} + \not{k}) \gamma^- (\not{p} - \not{q}) \gamma_\nu \not{p} \gamma^- (\not{p} + \not{k}) \quad (21)$$

with $k^- = 0$, $q^+ = 0$, $p^- = zq^-$ and

$$p^+ = -\frac{(p_t - q_t)^2}{2(1-z)q^-} \quad k^+ = -p^+ + \frac{(p_t + k_t)^2}{2zq^-} \quad (22)$$

It is customary to write the hadronic tensor in terms of Lorenz invariant functions W_1, W_2, W_3 defined as [18]

$$M_h W_{\mu\nu} \equiv -(g_{\mu\nu} - \frac{q_\mu q_\nu}{q^2}) F_1 + \frac{1}{P \cdot q} (P_\mu - \frac{q_\mu P \cdot q}{q^2}) (P_\nu - \frac{q_\nu P \cdot q}{q^2}) F_2 + i \epsilon_{\mu\nu\rho\sigma} \frac{P^\rho q^\sigma}{P \cdot q} F_3 \quad (23)$$

where the structure functions are defined as $F_1 = M_h W_1$, $F_2 = \nu W_2$ and $F_3 = \nu W_3$ with M_h being the target nucleon mass and $P \cdot q = M_h \nu$. The differential cross section $d\sigma/dxdQ^2$ can be written in terms of the structure functions as

$$\frac{d\sigma}{dxdQ^2} = \frac{1}{2\pi} \frac{G_F^2}{x [1 + \frac{Q^2}{M_W^2}]^2} \left\{ y^2 x F_1 + (1-y) F_2 + y \left[1 - \frac{y}{2}\right] x F_3 \right\} \quad (24)$$

which are related to the hadronic tensor via

$$\begin{aligned}
F_1 &= -\frac{1}{2} \left[g^{\mu\nu} + \frac{q^2}{(q \cdot P)^2} P^\mu P^\nu \right] M_h W_{\mu\nu} \\
F_2 &= \frac{q^2}{2q \cdot P} \left[g^{\mu\nu} + 3 \frac{q^2}{(q \cdot P)^2} P^\mu P^\nu \right] M_h W_{\mu\nu} \\
F_3 &= \Pi^{\mu\nu} M_h W_{\mu\nu}
\end{aligned} \tag{25}$$

where

$$\Pi^{\mu\nu} = -i \epsilon^{\mu\nu\alpha\beta} \frac{P_\alpha q_\beta}{2P \cdot q} \tag{26}$$

To give explicit expressions for the structure functions, we need to evaluate the traces². This has already been done for the case of W^{++} and W^{--} in [17]. Using $K'_0 = -K_1$ and the identity

$$\int_0^\infty dp \frac{p J_0(p r_t)}{[p^2 + a^2]} \equiv K_0(a r_t) \tag{27}$$

gives

$$\begin{aligned}
2xF_1 &= \frac{N_c \sigma Q^2}{4\pi^3} \int_0^1 dz \int dr_t^2 \gamma(x, r_t) \{ a^2 [z^2 + (1-z)^2] K_1^2(a r_t) \} \\
F_2 &= \frac{N_c \sigma Q^2}{4\pi^3} \int_0^1 dz \int dr_t^2 \gamma(x, r_t) \left\{ 4z^2(1-z)^2 Q^2 K_0^2(a r_t) + a^2 [z^2 + (1-z)^2] K_1^2(a r_t) \right\} \\
xF_3 &= \frac{N_c \sigma Q^2}{4\pi^3} \int_0^1 dz \int dr_t^2 \gamma(x, r_t) \left\{ (1-2z) a^2 K_1^2(a r_t) \right\}
\end{aligned} \tag{28}$$

with $a^2 \equiv z(1-z)Q^2$ and K_0 and K_1 are the modified Bessel functions. Using these expressions for the structure functions in (24) and (4) gives the all twist cross section for $\nu N \rightarrow \mu X$. The structure functions F_1 and F_2 are the same as those for electron nucleon deep inelastic scattering while F_3 is specific to neutrino interactions. In the kinematics of interest here (high energy or small x), F_3 vanishes as can be checked explicitly by doing the z integration in (28).

One can distinguish three distinct kinematical regions in which the neutrino nucleon total cross section has a different behavior. In the very high energy limit where unitarity effects are dominant ($Q_s \geq M_W$), the cross section is given by (28). This is the saturation region and the total cross section grows much more slowly (compared to the perturbative power growth) due to high gluon density effects. At lower energies where Q_s^2 and Q_{max}^2 , as defined in (1), are both much less than M_W^2 , one can use the standard perturbative results

²We would like to thank W. Vogelsang for his help with evaluating these traces.

to which our expressions reduce³. The most interesting region is at high energies (but not too high where unitarity effects are dominant) where $Q_s^2 \ll M_W^2$ but $Q_{max}^2 > M_W^2$. Here, we are in the geometric scaling region where high gluon density effects lead to an enhancement of the unitarized cross section. We discuss this enhancement in the next section.

3 Enhancement of neutrino-nucleon cross section

Geometric scaling was first observed at HERA for the virtual photon nucleon total cross section [10]. Roughly speaking, geometric scaling is the phenomenon that DIS structure functions depend on only one variable $\tau \equiv Q^2/Q_s^2(x)$ rather than two independent variables x and Q^2 . Geometric scaling arises naturally from the all twist formulation of small x QCD [12, 13]. It has been shown that geometric scaling is a property of the non-linear generalizations of the QCD evolution equation for the dipole cross section at small x in the region where $Q^2 < Q_s^2$. More interestingly, it has been recently shown that the scaling region extends far beyond the saturation region [14, 15], contrary to naive expectations (see Fig. 3). The dipole cross section is the universal building block which is also present in the unitarized all twist cross sections for particle production in pA collisions [19].

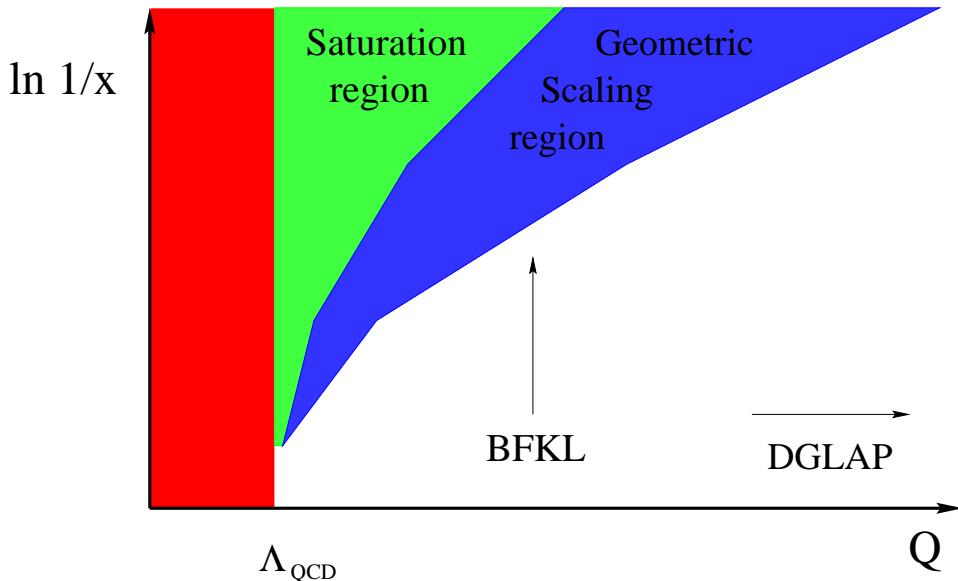


Figure 3: The saturation region.

To make an estimate of this enhancement factor for ultra high energy neutrinos, we need to know the dipole cross section $\gamma(x, r_t, b_t)$ beyond the classical approximation. In principle, one can determine $\gamma(x, r_t, b_t)$ from the renormalization group equations derived in [12]. In this approach, one solves the non-linear renormalization group equations on a lattice which can then be used to calculate the proton structure function F_2 which shows

³See [17] for a discussion of the high Q^2 limit of all twist calculations.

good agreement with the HERA data [20] at not very high Q^2 . To improve the high Q^2 behavior, one needs to include DGLAP evolution into the non-linear evolution equations. This is a very difficult problem which has not been solved yet. Alternatively, one can model the dipole cross section. One such model that includes DGLAP evolution is due to Bartels, Golec-Biernat and Kowalski [11]. In this model, the dipole cross section is given by

$$\gamma(x, r_t, b_t) = \left[1 - \exp[-\pi^2 \alpha_s r_t^2 x G(x, \mu^2)/3\sigma_0] \right] \quad (29)$$

with $\mu^2 = C/r_t^2 + \mu_0^2$ and $\sigma_0 = 23$ mb. This parametrization of the dipole cross section is used by [11] to successfully fit all HERA data on inclusive and diffractive structure functions below $x = 0.01$ and at all Q^2 . However, this model will not have the enhancement since it still uses the DGLAP form of the dipole cross section at small r_t ($\gamma(x, r_t, b_t) \sim r_t^2 Q_s^2$).

One can also use the BFKL formalism to calculate the dipole cross section in the geometric scaling region. This was done in [21] where both LO and NLO BFKL evolution equations were used and a resummation of most important collinear (and anticollinear) divergences was performed. In this formalism, the dipole cross section in the geometric scaling region is given by

$$\gamma(x, r_t, b_t) = \left[r_t^2 Q_s^2(x) \right]^{1-\gamma_s} \exp \left\{ - \frac{1}{2\beta\bar{\alpha}_s \log 1/x} \left[\log[1/r_t^2 Q_s^2(x)] \right]^2 \right\} \quad (30)$$

where $\bar{\alpha}_s = \frac{N_c \alpha_s}{\pi}$ and $\beta = 34$. A LO BFKL analysis leads to $1 - \gamma_s = 0.644$ while NLO BFKL leads to only a small change in this number. It is shown that the functional form of the saturation scale Q_s^2 depends on the energy considered. In the x range of relevance here, however, it is a good approximation to use $Q_s^2(x) = \Lambda^2 e^{\lambda_s \log 1/x}$ with $\lambda_s \sim 0.28$ and $\Lambda \sim 200$ MeV.

A more desirable model would interpolate between the saturation region and the geometric scaling region and have the DGLAP anomalous dimension in the high Q^2 region. An ansatz for the dipole cross section is given in [22] which interpolates between the saturation region and the geometric scaling region and fits the HERA data at low Q^2 [23]. Work is in progress [24] to improve this ansatz by including DGLAP evolution. It should be emphasized that the leading twist high energy neutrino cross sections are dominated by a single scale $Q \sim M_W$ so that there is very little evolution in Q^2 while there is significant evolution in x (by orders of magnitude!) so that it is essential to treat the small x evolution consistently.

In what follows, we will use the dipole cross section from the BFKL approach with the effects of gluon saturation in the boundary between the saturation region and the geometric scaling region taken into account, as given in (30), to make a rough numerical estimate of the enhancement factor. We will consider the ratio of the dipole cross section in the coordinate space calculated from the standard leading twist DGLAP evolution with anomalous dimension⁴ of 1 and the dipole cross section calculated from the BFKL approach with

⁴The definition of anomalous dimension is not standard. In our notation, the anomalous dimension is $1 - \gamma_s$ so that the DGLAP anomalous dimension is 1.

the saturation effects taken into account in the Geometric scaling region. The normalized dipole cross section (divided by a hadronic size σ_0 to make it dimensionless) is given by $[r_t^2 Q_s^2]$ in the standard leading twist approach and by $[r_t^2 Q_s^2]^{1-\gamma_0}$ in the BFKL approach (ignoring the exponential term which is very close to unity) with the high gluon density effects taken into account in the boundary [21]. Setting $r_t \sim 1/M_W$ since the cross section is dominated by M_W , the ratio of cross sections in the geometric scaling region is

$$\left[\frac{M_W^2}{Q_s^2(x)} \right]^{\gamma_s} \sim 10 \quad (31)$$

with $Q_s^2(x \sim 10^{-7}) \sim 10 \text{ GeV}^2$ and $\gamma_s = 0.36$. One might think that this enhancement is due to the fact that BFKL cross sections grow faster than DGLAP cross sections. However, this is not the case. It is easy to show that the ratio of cross sections from the BFKL approach with and without geometric scaling is still larger than one (this ratio is about 3, with choice of the infrared cutoff $k_0^2 = 1 \text{ GeV}^2$ [7] in the BFKL approach without gluon saturation effects in the boundary) so that the enhancement is due to the geometric scaling. Since different values of x contribute to the cross section, one will have different enhancement factors. This illustrates the fact that the neutrino nucleon cross section is enhanced in some neutrino energy range due to the geometric scaling property of the unitarized cross sections.

Off course, this is a very rough estimate but the enhancement should be robust. In a quantitative analysis, one will have to include contributions from different regions of x where one may or may not be in the geometric scaling region. At some neutrino energies, the dominant contribution will come from x 's where we will be fully in the geometric scaling region and the enhancement will be maximal⁵. As one goes to yet higher energies, the geometric scaling region shrinks due to the fact that $Q_s^2 \rightarrow M_W^2$ and one approaches the saturation region where unitarity effects become more important and eventually suppress the cross section compared to the leading twist cross section. A more quantitative analysis is in progress and will be reported elsewhere.

4 Discussion

We have calculated the total cross section for neutrino nucleon scattering via the charged current exchange including the high gluon density (higher twist) effects. We have shown that this cross section is expressed in terms of the dipole nucleon cross section which is the universal object appearing in all twist cross sections [19]. Using our expressions for the neutrino nucleon cross section and some model of the dipole nucleon cross section (given for example in [11]), one can estimate at what neutrino energies protons will look black to neutrinos (the black disk limit). This turns out to be at neutrino energies of $E_\nu \sim 10^{18}$ GeV. This may be too high of an energy for this effect to be observable in the near future.

⁵We are implicitly assuming that the cross section is dominated by $Q \sim M_W$ even in the geometric scaling region. It is possible that the effective Q will shift to smaller values but this will make the enhancement even stronger.

A more interesting effect happens at much smaller energies than the black disk limit. As shown here, the geometric scaling region extends all the way up to and beyond the weak boson mass already at neutrino energies of $E_\nu > O(10^{12})$ GeV. Therefore neutrino nucleon cross sections at these energies will be dominated by scales that are within the geometric scaling region where cross sections are typically enhanced. This enhancement factor can be as large as 1 – 2 orders of magnitude at $E_\nu > 10^{12}$ GeV. This will have very interesting consequences for neutrino astronomy and cosmology [25].

This enhancement will be important for the current and future neutrino observatories [25], [26], [27], [28], [29], [30]. It will be very interesting to see whether the observed cosmic ray data points beyond the GZK cutoff [31] are due to neutrinos [32]. For these events to be neutrinos with their cross sections enhanced due to geometric scaling requires a very large enhancement factor already at $E_\nu \sim 10^{11-12}$ where the data points are [26]. Several experiments will detect neutrinos through their horizontal air showers in the Earth's atmosphere due to neutrino air interactions whose rate will increase if the neutrino nucleon cross section is enhanced. On the other hand, the rate of up-going air showers initiated by the leptons produced in neutrino nucleon interactions will decrease if the neutrino nucleon cross section is enhanced since the Earth will be less transparent to neutrinos. A better understanding of the neutrino nucleon total cross section is essential to these experiments which will help clarify the origins of ultrahigh energy neutrinos.

Acknowledgments

We would like to thank A. Dumitru, R. Harlander, K. Itakura, D. Kharzeev, W. Kilgore, S. Kretzer, A. Stasto, D. Teaney, D. Triantafyllopoulos, R. Venugopalan and W. Vogelsang for useful discussions. We would also like to thank L. McLerran for pointing out to us the importance of geometric scaling and its role in the enhancement of cross sections and many illuminating discussions. This work is supported by the U.S. Department of Energy under Contract No. DE-AC02-98CH10886 and in part by a PDF from BSA.

References

- [1] For a review, see for example, F. Halzen, *Phys. Rep.* **333**, 349 (2000).
- [2] G.M. Frichter, D.W. McKay and J.P. Ralston, *Phys. Rev. Lett.* **74**, 1508 (1995); J.P. Ralston, D.W. McKay and G.M. Frichter, astro-ph/9606008; R. Gandhi, C. Quigg, M.H. Reno and I. Sarcevic, *Astropart. Phys.* **5**, 81 (1996); *Phys. Rev.* **D58**, 093009 (1998); M. Glück, S. Kretzer and E. Reya, *Astropart. Phys.* **11**, 327 (1999); J. Kwiecinski, A.D. Martin and A.M. Stasto, *Phys. Rev.* **D59**, 093002 (1999).
- [3] H.L. Lai *et al.*, CTEQ Collab., *Eur. Phys. J.* **C12**, 375 (2000); M. Glück, E. Reya and A. Vogt, *Eur. Phys. J.* **C5**, 461 (1998); A.D. Martin, R.G. Roberts, W.J. Stirling, and R.S. Thorne, *Eur. Phys. J.* **C4**, 463 (1998).
- [4] H1 Collab.: I. Abt *et al.*, *Nucl. Phys.* **B407**, 515 (1993); T. Ahmed *et al.*, *ibid.* **B439**, 471 (1995); S. Aid *et al.*, *Phys. Lett.* **B354**, 494 (1995); ZEUS Collab.: M. Derrick *et al.*, *Phys. Lett.* **B316**, 412 (1993), *Z. Phys.* **C65**, 379 (1995), *Phys. Lett.* **B345**, 576 (1995); T. Ahmed *et al.*, H1 Collab., *Phys. Lett.* **B324**, 241 (1994).
- [5] D. A. Dicus, S. Kretzer, W. W. Repko and C. Schmidt, *Phys. Lett. B* **514**, 103 (2001).

- [6] M. H. Reno, I. Sarcevic, G. Sterman, M. Stratmann and W. Vogelsang, hep-ph/0110235.
- [7] J. Kwiecinski, A. D. Martin and A. M. Stasto, *Acta Phys. Polon. B* **31**, 1273 (2000), *Phys. Rev. D* **59**, 093002 (1999).
- [8] M. Gluck, S. Kretzer and E. Reya, *Astropart. Phys.* **11**, 327 (1999).
- [9] L. Gribov, E. Levin and M. Ryskin, *Nucl. Phys.* **B188**, 555 (1981); A.H. Mueller and J. Qiu, *Nucl. Phys.* **B268**, 427 (1986); J. Jalilian-Marian, A. Kovner, L. McLerran and H. Weigert, *Phys. Rev.* **D55**, 5414 (1997).
- [10] A. M. Stasto, K. Golec-Biernat and J. Kwiecinski, *Phys. Rev. Lett.* **86**, 596 (2001).
- [11] K. Golec-Biernat and M. Wüsthoff, *Eur. Phys. J.* **C20**, 313 (2001), *Phys. Rev.* **D60**, 114023 (1999), *Phys. Rev.* **D59**, 014017 (1998); J. Bartels, K. Golec-Biernat and H. Kowalski, *Phys. Rev. D* **66**, 014001 (2002).
- [12] L. D. McLerran and R. Venugopalan, *Phys. Rev. D* **49**, 2233 (1994), *Phys. Rev. D* **49**, 3352 (1994); Y. Kovchegov, *Phys. Rev. D* **54**, 5463 (1996), *Phys. Rev. D* **55**, 5445 (1997), *Phys. Rev. D* **60**, 034008 (1999), *Phys. Rev. D* **61**, 074018 (2000); A. Ayala, J. Jalilian-Marian, L. D. McLerran and R. Venugopalan, *Phys. Rev. D* **52**, 2935 (1995), *Phys. Rev. D* **53**, 458 (1996); J. Jalilian-Marian, A. Kovner, A. Leonidov and H. Weigert, *Nucl. Phys. B* **504**, 415 (1997), *Phys. Rev. D* **59**, 014014 (1999), *Phys. Rev. D* **59**, 034007 (1999), [Erratum-ibid. *D* **59**, 099903 (1999)]; J. Jalilian-Marian, A. Kovner and H. Weigert, *Phys. Rev. D* **59**, 014015 (1999); A. Kovner, J. G. Milhano and H. Weigert, *Phys. Rev. D* **62**, 114005 (2000); A. Kovner and J. G. Milhano, *Phys. Rev. D* **61**, 014012 (2000); E. Iancu, A. Leonidov and L. D. McLerran, *Nucl. Phys. A* **692**, 583 (2001), hep-ph/0202270, *Phys. Lett. B* **510**, 133 (2001); E. Iancu and L. D. McLerran, *Phys. Lett. B* **510**, 145 (2001); E. Ferreira, E. Iancu, A. Leonidov and L. McLerran, *Nucl. Phys. A* **703**, 489 (2002).
- [13] I. Balitsky, *Nucl. Phys. B* **463**, 99 (1996), *Phys. Rev. Lett.* **81**, 2024 (1998), *Phys. Rev. D* **60**, 014020 (1999), *Phys. Lett. B* **518**, 235 (2001).
- [14] E. Iancu, K. Itakura and L. McLerran, *Nucl. Phys. A* **708**, 327 (2002), hep-ph/0205198.
- [15] J. Kwiecinski and A. M. Stasto, *Phys. Rev. D* **66**, 014013 (2002).
- [16] D. Kharzeev, E. Levin and L. McLerran, *Phys. Lett. B* **561**, 93 (2003).
- [17] L. McLerran and R. Venugopalan, *Phys. Rev.* **D59**, 094002 (1999); R. Venugopalan, *Acta Phys. Polon. B* **30**, 3731 (1999).
- [18] R. G. Roberts, “The structure of the proton”, Cambridge University Press, 1993.
- [19] A. Dumitru and J. Jalilian-Marian, *Phys. Lett. B* **547**, 15 (2002), *Phys. Rev. Lett.* **89**, 022301 (2002); F. Gelis and J. Jalilian-Marian, *Phys. Rev. D* **66**, 014021 (2002), *Phys. Rev. D* **66**, 094014 (2002), *Phys. Rev. D* **67**, 074019 (2003).
- [20] H. Weigert, Private communication.
- [21] A. H. Mueller and D. N. Triantafyllopoulos, *Nucl. Phys. B* **640**, 331 (2002); D. N. Triantafyllopoulos, *Nucl. Phys. B* **648**, 293 (2003).
- [22] E. Iancu, K. Itakura and L. McLerran, hep-ph/0212123.

- [23] E. Iancu, private communications.
- [24] F. Gelis, and J. Jalilian-Marian, work in progress.
- [25] A. Kusenko, hep-ph/0203002, hep-ph/0212232; A. Kusenko and T. J. Weiler, Phys. Rev. Lett. **88**, 161101 (2002).
- [26] <http://www-akeno.icrr.u-tokyo.ac.jp/AGASA/>
- [27] <http://www.auger.org>
- [28] <http://hires.physics.utah.edu>
- [29] <http://ifcai.pa.cnr.it/ifcai/euso.html>
- [30] <http://owl.gsfc.nasa.gov>
- [31] G. T. Zatsepin and V. A. Kuzmin, JETP Lett. **4**, 78 (1966) [Pisma Zh. Eksp. Teor. Fiz. **4**, 114 (1966)]; K. Greisen, Phys. Rev. Lett. **16** (1966) 748.
- [32] T. J. Weiler, AIP Conf. Proc. **579**, 58 (2001), hep-ph/0103023.